Influence of PS-*b*-PEO Diblock Copolymers on the Compatibility of Syndiotactic Polystyrene Modified Epoxy Blends

A. Tercjak, E. Serrano, M. D. Martin, C. Marieta, I. Mondragon

Escuela Universitaria Politécnica, Dpto. Ingeniería Química y Medio Ambiente, Universidad del País Vasco/Euskal Herriko Unibertsitatea, Pza. Europa, 1. 20018-Donostia/San Sebastián, Spain

Received 29 August 2005; accepted 5 February 2006
DOI 10.1002/app.24204
Published online in Wiley InterScience (www.interscience.wiley.com).

ABSTRACT: Homogeneous solutions of syndiotactic polystyrene (sPS) in diglycidylether of bisphenol A (DGEBA), containing 2.5, 5 and 7.5 wt % of thermoplastic with or without 0.5 and 1 wt % of poly(styrene-*b*-ethylene oxide) (PS-*b*-PEO) block copolymer, were polymerized using a stoichiometric amount of an aromatic amine hardener, 4,4′-methylene bis (3-chloro-2,6-diethylaniline) (MCDEA). The dynamic-mechanical properties and morphological changes of sPS-(DGEBA/MCDEA) compatibilized with different amount of PS-*b*-PEO have been investigated in this paper. The addition of the block copolymer produced significant changes in the morphologies generated. The size of the dispersed spherical sPS spherulites does not change significantly, but less spherulites of sPS appeared upon network formation in the systems with compatibilizer, what means that addition of compatibilizer in this system delayed crystallization of sPS in sPS-(DGEBA/MCDEA) systems and change phase separation mechanism from crystallization-induced phase separation (CIPS) and reaction-induced phase separation (RIPS) almost only to RIPS. Moreover, PS-*b*-PEO with higher molecular weight of PS block seems to be a more effective compatibilizer than one with lower molecular weight of PS block. © 2006 Wiley Periodicals, Inc. J Appl Polym Sci 102: 479–488, 2006

Key words: syndiotactic polystyrene; compatibility; morphology; diblock copolymer; dynamic–mechanical properties

INTRODUCTION

Syndiotactic polystyrene (sPS) is a semicrystalline polymer, which has attracted much interest due to several physical properties. The most important properties of sPS are high modulus of elasticity and heat resistance, low dielectric constant, excellent resistance to chemicals because of its stereoregularity, and relatively fast crystallization rate.[1] sPS has gained increasing academic and industrial interests since its first successful synthesis in 1985 using a titanium metallocene catalyst as reported by Ishihara et al.[2] However, because sPS has some disadvantages such as low strength[3] and high processing temperature,[4] it has been restricted to a few applications. One way to overcome these problems is blending sPS with other thermoplastic polymers, such as poly(vinyl methyl ether) (PVME),[5–7] poly(2,6-dimethyl-1,4-phenyle oxide) (PPO),[8,9] poly(*p*-phenylene sulfide) (PPS),[10] atactic polystyrene (aPS),[11–14] or with epoxy/amine systems.[15–19] Blending of polymers provide an efficient way of developing new materials with tailored properties but most of polymer blends are immiscible at molecular level. The incompatibility between polymeric pairs is responsible for poor mechanical properties of those blends due to poor interfacial adhesion between separated phases. Therefore, the modification concept using compatibilizers has been investigated to obtain polymer blends with more desirable properties. One of the most commonly used methods is to add a third component that is totally or partially miscible (or at least compatible) with both homopolymer phases. The component may be a suitable block or graft copolymer or functional polymer, which are capable of acting as interfacial agents.[20] It is well known that block copolymers can be effective compatibilizers for immiscible polymer blends containing sPS[21–27] or epoxy resins.[28,29]

Theoretical works[20,30–33] have shown that block copolymers prefer to locate at the interface reducing the interfacial tension. The localization of the block copolymer at the interface, with the block extending into their respective homopolymer phases, not only minimizes the contact between the unlike segments of the copolymer and homopolymer but also displaces the

Correspondence to: I. Mondragon (iapmoegi@sc.ehu.es).
Contract grant sponsor: POLYNETSET, Research Training Network (RTN) program, European Commission; contract grant number: HPRN-CT-2000–00,146.
Contract grant sponsor: Ministerio de Ciencia y Tecnología (Spain); contract grant number: MAT 2001–0714.

two homopolymers away from the interface, thereby decreasing the enthalpy of mixing between the homopolymers.[34] As a consequence, the block copolymers at interface are expected to stabilize morphology against coalescence.[35] In other words, the copolymer is believed to play a role of an emulsifier, thus controlling dispersed particle size and interfacial adhesion.

Owing to the polarities of sPS and epoxy resin, mixtures are immiscible because of lack of specific interactions between these both two polymers and two-phase morphology with poor interfacial adhesion is developed. Previous work[18,19] has reported results on the phase separation and crystallization of the thermoset precursor upon curing in the presence of different sPS contents. Taking into account the obtained results, adding suitable block copolymer to induce compatibilization between sPS and epoxy during curing process can be of interest. In the present study, a poly(styrene-*b*-ethylene oxide) (PS-*b*-PEO) diblock copolymer has been used as compatibilizer. It was chosen taking into account both the difficulty in synthesis of diblock copolymer containing sPS block and miscibility between sPS and aPS.[11–14]

This work aims to examine the effect of adding small amounts of PS-*b*-PEO on dynamic–mechanical properties and morphologies in sPS-(epoxy/amine) blends. The effect of molecular weight of diblock copolymer on the miscibility of these blends has also been studied.

EXPERIMENTAL PART

Materials and sample preparation

In this study, the epoxy system consisted of a diglycidyl ether of bisphenol A (DGEBA), gently supplied by Dow Chemicals (Rheinmünster, Germany), was cured with a stoichiometric amount of an aromatic amine hardener, 4,4′-methylene bis(3-chloro-2,6-diethylaniline) (MCDEA), kindly supplied by Lonza (Basel, Germany). The semicrystalline thermoplastic modifier used was syndiotactic polystyrene (sPS), provided by Dow Chemicals (DCG Buna Sow Luena Olefinverbund GmbH, Basel, Germany), known under the trade name Questra QA 101, with number-average molecular weight of 94,000 g mol^{-1}. Two diblock copolymers of poly(styrene-*b*-ethylene oxide) (PS-*b*-PEO), obtained from Polymer Source (Montreal, Canada), were used as compatibilizers, one with number-average molecular weights 125,000 and 16,100 g mol^{-1} and the other with 58,600 and 31,000 g mol^{-1} for sPS and PEO blocks, respectively. M_w/M_n for the first one was 1.04 and for the second one was 1.03, which will be denoted HBC (block copolymer with higher molecular weight of PS block) and LBC (block copolymer with lower molecular weight of PS block), respectively, along this text.

sPS-(DGEBA/MCDEA) mixtures were prepared by following the procedure used by Schut et al.[36] Prior to mixing, sPS pellets were powdered and dried overnight at 80°C in an air oven. Subsequently, sPS-DGEBA mixtures containing different sPS weight percentages (2.5, 5, and 7.5 wt %) and different PS-*b*-PEO weight percentages (0.25, 0.5, and 1 wt %) were prepared by dispersing a weighed amount of sPS and PS-*b*-PEO in DGEBA at 220°C in an oil bath under continuous stirring for 10 min. Then, mixtures were moved to a Wood's metal bath at 290°C and stirred for other 10 min until complete dissolution of both sPS and PS-*b*-PEO. Simultaneously, MCDEA was melted in another test tube at 220°C for 5 min. Finally, the molten MCDEA was added to the sPS-(PS-*b*-PEO)-DGEBA mixtures cooled down to 220°C and stirred for 30 s. The samples were then cured for 2 h at 220°C.

Techniques

Dynamic mechanical analysis (DMA) of the specimens was conducted using a Perkin–Elmer DMA 7e apparatus at the frequency of 1 Hz in a three-point device. The temperature range studied was from 30 to 250°C at a heating rate of 5°C min^{-1}, using $24 \times 3 \times 1$ mm^3 specimens. During the scan, the samples were subjected to a static force of 110 m*N* and a dynamic force of 100 m*N*.

Calorimetric measurements were performed in a Mettler Toledo DSC 822 differential scanning calorimeter equipped with a Sample Robot TSO 801 RO. Nitrogen was used as a purge gas (10 mL min^{-1}). Temperature and enthalpy were calibrated by using an indium standard. Measurements were performed in sealed aluminum pans containing a sample weight of around 10 mg. To ensure comparable thermal history, all samples were first heated to 300°C and were maintained at that temperature for 10 min, then cooled down to 30°C and reheated to 300°C, all at a rate of 10°C min^{-1}. The crystallization temperature (T_c) was taken as the minimum of exothermic peak, whereas the melting point temperature (T_m) was taken as the maximum of the endothermic transition.

The morphology of selected blends was examined by SEM using a JEOL 6400 microscope at an accelerating voltage of 15 kV. The samples were fractured under cryogenic conditions using liquid nitrogen. The cryogenically fractured surface of the molded specimens was coated with thin layers of gold of about 100 Å before SEM examination.

AFM topography images of the cryogenic fracture surfaces of cured blends were recorded in tapping mode at room temperature by using a scanning probe microscope (SPM) (Nanoscope IIIa, Multimode™ from Digital Instruments). Etched single beam cantilever (225 μm length) silicon nitride probes having a tip's nominal radius of curvature of 5–10 nm were

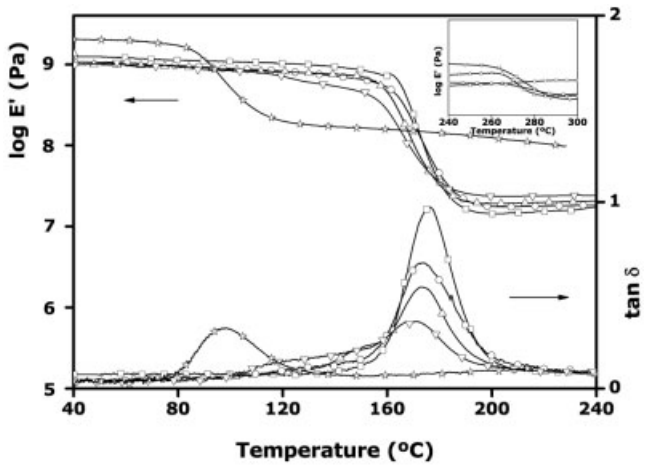

Figure 1 Storage modulus, E', and loss factor, tan δ, versus temperature of sPS-(DGEBA/MCDEA) blends containing different amounts of sPS: (-□-), neat DGEBA/MCDEA; (-○-), 2.5 wt % sPS; (-△-), 5 wt % sPS; (-▽-), 7.5 wt % sPS; (-☆-), neat sPS. The inset shows E' versus temperature curves at high temperature range.

used. Scan rates ranged from 0.8 to 1.6 Hz s^{-1}. The sample line was 512 and the target amplitude was around 0.7 V. Height and phase images were recorded simultaneously during scanning. To obtain repeatable results of blend morphologies, different regions of the specimens were scanned. Similar images were obtained, thus demonstrating the reproducibility of the results.

RESULTS AND DISCUSSION

Dynamic mechanical analysis is a powerful tool for investigating miscibility relations in polymer blends. The loss factor, tan δ, temperature dependence indicates changes in the molecular mobility from localized skeleton motions in the subglass region to segmental motions at the glass transition. The α relaxation maximum of the loss tangent curve, if accompanied by a maximum at the loss modulus E'' curve, testifies the glass transition and is often identified with the glass temperature. Miscibility of polymers, occurring in the amorphous phase, is determined by a single glass temperature (T_g), which increases monotonically as a function of composition. Immiscible blends are characterized by separate glass transition temperatures of individual polymers. Blends with some degree of miscibility show separate glass temperatures, but shifted toward each other.

The temperature dependence of tan δ and storage modulus, E', for sPS-(DGEBA/MCDEA) blends without compatibilizer is shown in Figure 1. The respective T_gs of neat sPS and DGEBA/MCDEA are 107 and 176°C. For these blends without PS-*b*-PEO, two distinct tan δ peaks are discernible. The lower one corresponds to the T_g of the dispersed sPS-rich phase [around 119 and 120°C for 2.5 and 5 wt % sPS-(DGEBA/MCDEA), respectively] and the peak at about 172°C corresponds to the T_g of DGEBA/MCDEA-rich matrix.

The presence of two peaks in the blends thus indicates that polymers are immiscible in amorphous phase. The storage modulus values of the sPS-(DGEBA/MCDEA) blends have the same tendency as for neat DGEBA/MCDEA. The storage modulus drops in two orders of magnitude after overcoming the glass transition of DGEBA/MCDEA phase and shows a broad plateau up to ending the measurements. It is also worth to note that after relaxation of epoxy phase the systems modified with sPS have rubbery-like behavior, indicating maintenance of elastic properties of the system, which means that these systems are thermosetting materials with epoxy matrix. Additionally, rubbery modulus (E_r') values show insignificant, relatively low decrease in the softening of sPS phase, which depends on amount of sPS in blends (see inset of Fig. 1). After that the rubbery modulus values are still stable up to the end of measurement, thus confirming that in these blends, epoxy resin forms the matrix. The influence of the sPS phase on the E' curve can be observed only for blends containing 7.5 wt % sPS. In this case, E' decreases steadily but continuously when the T_g of the sPS phase is overcome. Moreover, the decrease of E' temperature dependence in the softening point of sPS phase is deeper than for blends containing less than 7.5 wt % sPS (see inset of the Fig. 1). Furthermore, it is clearly seen that the tan δ peaks of epoxy phase are higher than that for sPS phase in blends with 2.5 and 5 wt % sPS, so implying that sPS phase is the separated phase. For the blend containing 7.5 wt % sPS, even tan δ peak of epoxy phase is still higher than sPS phase, both peaks are broadened, indicating that cocontinuity occurs and a region of dual phase continuity exists.

The temperature dependencies of tan δ and E' for the blends containing 2.5 and 5 wt % sPS and different amounts of PS-*b*-PEO diblock copolymer with higher molecular weight of PS block (HBC) are shown in Figures 2 and 3, respectively. On addition of HBC to the blends, for the blends containing less than 1 wt % HBC, the T_g of epoxy-rich matrix is shifted to lower temperatures with increase of HBC (Figs. 2 and 3). Simultaneously, $E'(T)$ of those blends drops in two orders of magnitude after glass–rubber transition of DGEBA/MCDEA phase and after that shows plateau up to the end of measurement except a relatively low decrease of E' in the softening point of sPS phase (see inset of the Figs. 2 and 3). The values of E_r in case of the systems with block copolymer are higher than those without block copolymer. Both shifting T_g of DGEBA/MCDEA phase to lower temperature and higher $E_r'(T)$ could indicate that the miscibility be-

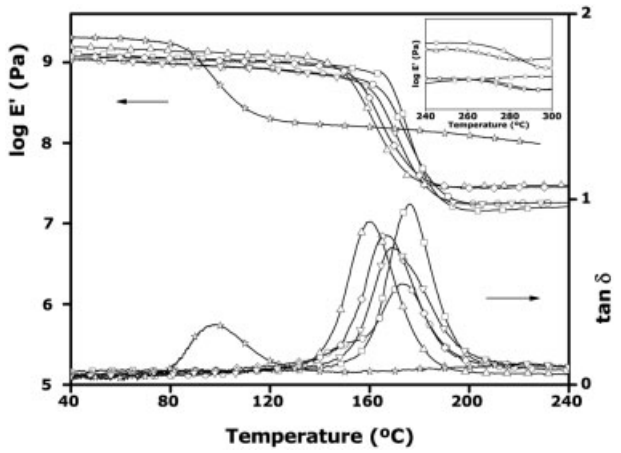

Figure 2 Storage modulus, E', and loss factor, tan δ, versus temperature for 2.5 wt % sPS-(DGEBA/MCDEA) blends modified with different amounts of PS-*b*-PEO (HBC): (-□-), neat DGEBA/MCDEA; (-○-), 0 wt %; (-◇-), 0.25 wt %; (-△-), 0.5 wt %; (-▽-), 1 wt %; (-☆-), neat sPS. The inset shows E' versus temperature curves at high temperature range.

tween sPS and DGEBA/MCDEA phases was improved. One can suppose that compatibilizer has migrated to the interface between the two phases of sPS-(DGEBA/MCDEA), thus enhancing the interaction between the two incompatible phases. Additionally, the height of the tan δ peaks for the system modified with PS-*b*-PEO is higher than that for systems without block copolymers. It can be because addition of compatibilizer to these systems hinders crystallization of sPS phase leading to a lack of the amount of sPS spherulites and, consequently, more amorphous sPS phase is microdispersed into the DGEBA/MCDEA matrix, which has higher molecular mobility. This can be explained by taking into account two facts. On one hand, as it was published in our previous study,[18] during curing of sPS-(DGEBA/MCDEA) systems at 220°C, both crystallization of sPS and epoxy polymerization reaction can induce phase separation (CIPS and RIPS, respectively). On the other hand, the addition of PS-*b*-PEO results in the compatibilization between sPS and epoxy-rich phase, because hydrogen bonds are formed between the hydroxyl groups of MCDEA cured epoxy and ether groups of PEO block[37,38] but also as a consequence of partial miscibility between PS block and sPS.[11–14] Taking this into account, less spherulites of sPS phase can be produced during phase separation, which occurs mostly by RIPS leading to more amorphous phase of sPS. It should also be pointed out that addition of 0.5 wt % HBC into 2.5 wt % sPS-(DGEBA/MCDEA) system means 20 wt % HBC comparing with weight percentage of sPS in blends and in case of 5 wt % sPS-(DGEBA/MCDEA) systems, it means 10 wt % HBC related to weight percentage of sPS. Consequently, 2.5 wt % sPS-(DGEBA/MCDEA) blends need higher amount of block copolymer with respect to sPS content in order that the compatibilization effect can be observed.

Introducing 1 wt % HBC into the blends reduced the compatibilization effect in sPS-HBC-(DGEBA/MCDEA) blends and did not show any significant changes in glass–rubber transition compared to the glass–rubber transition of the corresponding individual components (see Figs. 2 and 3). In this case, addition of 1 wt % into 2.5 wt % sPS-(DGEBA/MCDEA) system means 40 wt % HBC comparing with sPS content and for 5 wt % sPS-(DGEBA/MCDEA) system, it means 20 wt % HBC with respect to sPS content. As a consequence, HBC can not work only as a compatibilizer, thus both separation and compatibilization of HBC effects are in competition.

Additionally, the effect of molecular weight and adding amount of diblock copolymer on the miscibility of sPS-(DGEBA/MCDEA) system has also been studied. Temperature dependencies of tan δ and E' for the same sPS-(DGEBA/MCDEA) blends with diblock copolymers with two different molecular weights are plotted in Figure 4. The diblock copolymer with higher molecular weight of PS block (HBC) seems to be more effective in compatibilizing sPS-(DGEBA/MCDEA) blends than that with lower molecular weight (LBC). In case when HBC is used, the shifting range of T_g peak of DGEBA/MCDEA phase to low temperature is more obvious than that for blends containing LBC. The T_g peaks of DGEBA/MCDEA phase in blends with 0.5 wt % HBC are moved to 159.1 and 157.4°C for 2.5 and 5 wt % sPS, respectively. Addition of the same amount of LBC block copolymer to the blends shifted T_g peaks of epoxy phase to 173 and 164°C. Moreover, the magnitudes of $E'(T)$ dependence

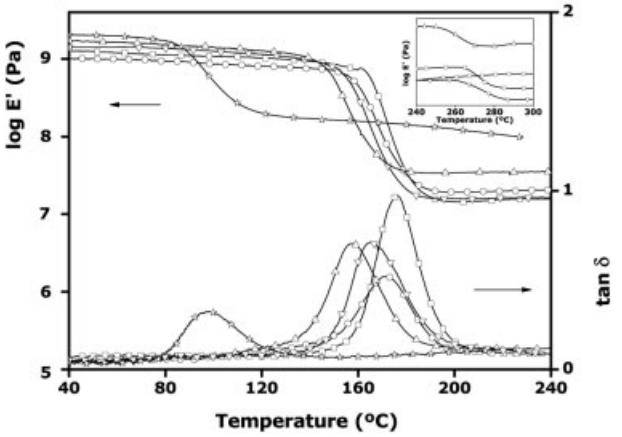

Figure 3 Storage modulus, E', and loss factor, tan δ, versus temperature for 5 wt % sPS-(DGEBA/MCDEA) blends modified with different amounts of PS-*b*-PEO (HBC): (-□-), neat DGEBA/MCDEA; (-○-), 0 wt %; (-△-), 0.5 wt %; (-▽-), 1 wt %; (-☆-), neat sPS. The inset shows E' versus temperature curves at high temperature range.

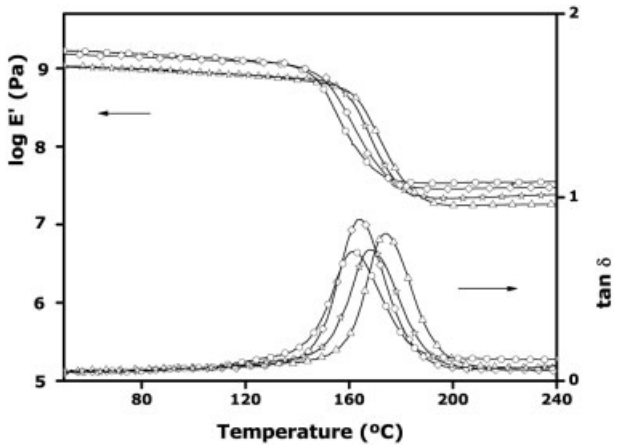

Figure 4 Storage modulus, E', and loss factor, tan δ, versus temperature for the sPS-(DGEBA/MCDEA) blends with different molecular weights of PS-*b*-PEO: (-◇-), 2.5 wt % sPS 0.5 wt % HBC; (-△-), 2.5 wt % sPS 0.5 wt % LBC; (-○-), 5 wt % sPS 0.5 wt % HBC; (-☆-), 5 wt % sPS 0.5 wt % LBC.

depend strongly on the amount and molecular weight of the compatibilizer. Blends containing HBC as compatibilizer, show higher E' magnitudes than the corresponding ones containing LBC.

DSC also is a useful tool for studying miscibility of blends, especially blends containing crystalline polymers. The DSC curves of the 5 wt % sPS-(DGEBA/MCDEA) without and with different amounts of HBC or LBC recorded during heating and cooling runs are presented in Figures 5 and 6, respectively. The parameters of the melting and crystallization of all investigated blends are summarized in Table I. The degree of crystallinity of the sPS phase in blends, X_c, was calculated from the melting enthalpy, ΔH_m, by the following equation:

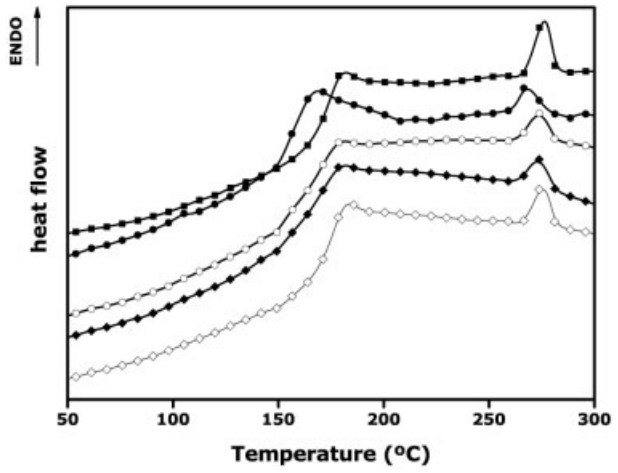

Figure 5 DSC melting curves of 5 wt % sPS-(DGEBA/MCDEA) blends without and with compatibilizer: (-■-), 0 wt %; (-●-), 0.5 wt % HBC; (-○-), 0.5 wt % LBC; (-◆-), 1 wt % HBC; (-◇-), 1 wt % LBC.

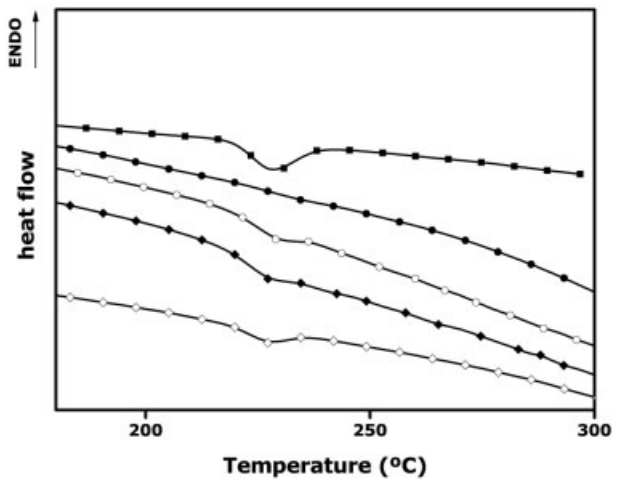

Figure 6 DSC crystallization curves of 5 wt % sPS-(DGEBA/MCDEA) blends without and with compatibilizer: (-■-), 0 wt %; (-●-), 0.5 wt % HBC; (-○-), 0.5 wt % LBC; (-◆-), 1 wt % HBC; (-◇-), 1 wt % LBC.

$$X_c = \frac{\Delta H_m}{\Delta H_m^0} \tag{1}$$

where ΔH_m^0, heat of fusion of 100% crystalline sPS, is 53 J/g.[39] The melting enthalpies of the sPS phase were recalculated in relation to the blend's weight composition.

Generally, addition of compatibilizers seems to have no influence on the T_m and T_c of crystalline sPS phase in the blends (see Figs. 5 and 6 and Table I). Both melting and crystallization of sPS phase in sPS-HBC-(DGEBA/MCDEA) or sPS-LBC-(DGEBA/MCDEA) systems occurred in temperature ranges close to

TABLE I
DSC Parameters of Melting and Crystallization of sPS-HBC-(DGEBA/MCDEA) and sPS-LBC-(DGEBA/MCDEA) Blends

sPS (wt%)	HBC (wt%)	LBC (wt%)	sPS phase		
			X_c (%)[a]	T_c (°C)	T_m (°C)
0					
			3.3	231.5	271.5
	0.25		2.1	228.5	269.4
2.5	0.5		—[b]	—[b]	—[b]
	1		1.6	231.0	269.7
	0.5	1.2	231.5	266.1	
	1	1.7	230.9	268.4	
			4.6	235.2	277.5
	0.5		1.7	—[b]	266.5
5	1		3.8	231.8	273.8
		0.5	2.6	230.7	274.3
		1	3.9	229.8	274.8
100			45.2	236.8	278.3

[a] Normalized crystallinity.
[b] No crystallization detected during experimental conditions.

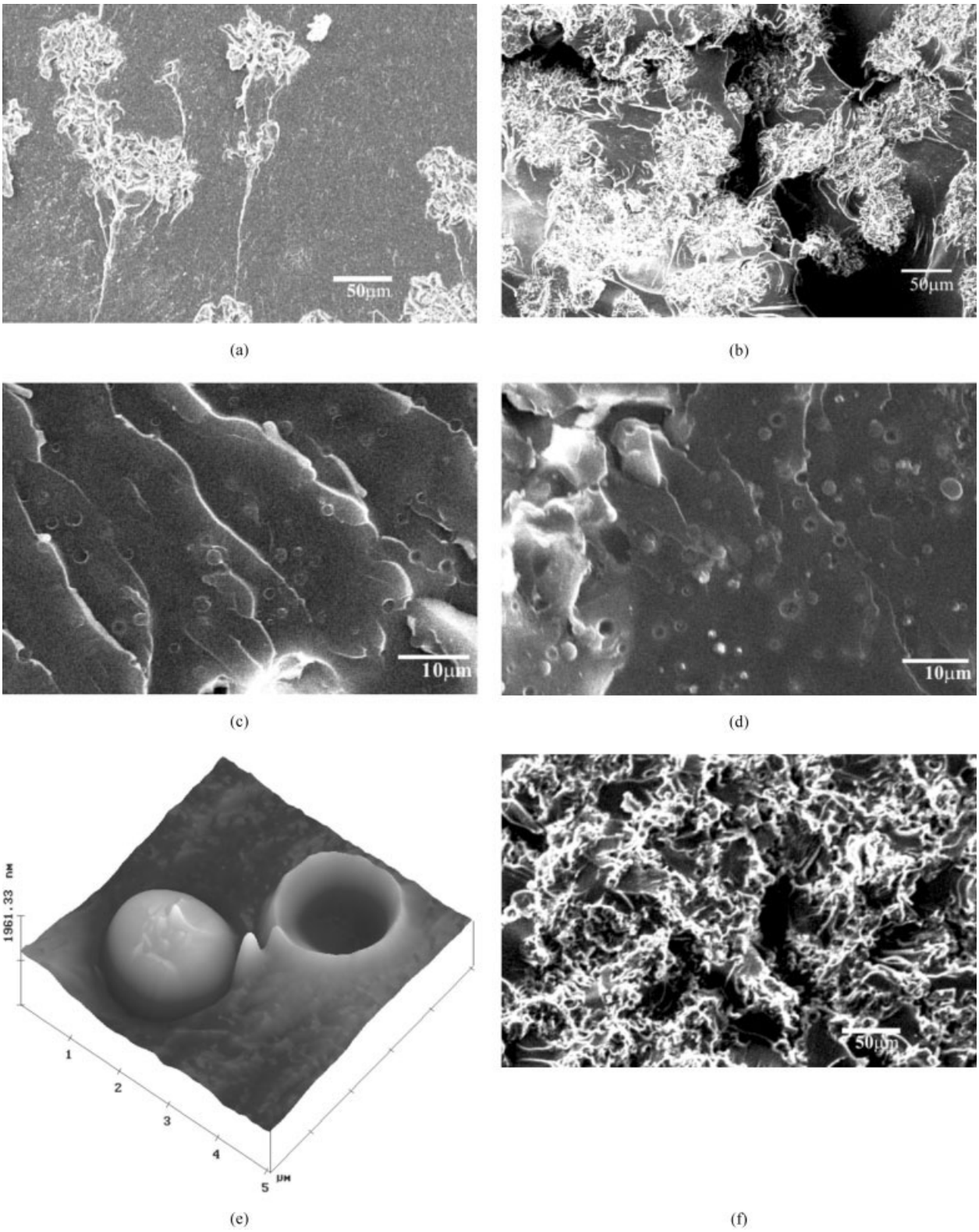

Figure 7 SEM and AFM micrographs of sPS-(DGEBA/MCDEA) cryo-fractured surface: (a) 2.5 wt % sPS (×300), (b) 5 wt % sPS (×300), (c) 2.5 wt % (×2000), (d) 5 wt % sPS (×2000), (e) 5 wt % sPS 3D AFM, (f) 7.5 wt % sPS (×300).

the corresponding temperature of the sPS phase in uncompatibilized blends. However, as presented in Table I, for the blend containing 2.5 wt % sPS and 0.5 wt % HBC, neither crystallization nor fusion has been detected during DSC experimental conditions, indicating that addition of HBC into these blend leads to a

lower tendency to crystallization of sPS phase. Similar behavior is observed for the blend with 5 wt % sPS and 0.5 wt % HBC (see Figs. 5 and 6 and Table I). The T_m of sPS phase in these blends is shifted to lower temperature and no crystallization exotherm is observed, indicating that crystallization of sPS phase in blends is hindered by addition of HBC as compatibilizer. Additionally, the X_c values of sPS phase in these systems are slightly lower than that of system without compatibilizer (see Table I). These results can be related to the increase of interfaces in blends, which leads to decrease of weight fraction of the bulk sPS. Taking into account both results obtained for sPS-(DGEBA/MCDEA) blends with 0.5 wt % HBC and the fact that addition of 0.25 or 1 wt % LBC do not change significantly melting endotherm and crystallization exotherm of sPS-(DGEBA/MCDEA) blends can be concluded that 0.5 wt % HBC is an optimal amount of HBC necessary to improve the compatibility between sPS and epoxy matrix phases. DSC results are in good agreement with DMA results shown above.

DSC data obtained for sPS-LBC-(DGBEA/MCDEA) blends suggested that introducing small amount of LBC to the blends do not lead to significant changes related to compatibility effect. Moreover, as has been reported by Ho et al.,[40] compatibilization effect occurs for molecular weight ratio between sPS and PS block lower than one. Taking this into account, we can speculate that blends compatibilized with PS-*b*-PEO with higher molecular weight work as surfactant because $M_{n,\mathrm{sPS}}/M_{n,\mathrm{PS}} = 94{,}000/125{,}000 \sim 0.75$, so as to create the shells of spherical microdomains of sPS phase in blends. Diblock copolymer with lower molecular weight forms phase-separated microdomains ($M_{n,\mathrm{sPS}}/M_{n,\mathrm{PS}} = 94{,}000/58{,}600 \sim 1.6$) having limitation in size due to the effect of compatibilization.

It can be also mentioned that higher molecular weight block copolymers would give higher interfacial adhesion due to deeper anchoring of each block into each of the phases. The influence of introduction of compatibilizer on the kinetics of crystallization in sPS-(DGEBA/MCDEA) systems will be reported in a forthcoming publication.

SEM and AFM observation was made on cryogenically fractured surfaces of the sPS-modified epoxy blends without and with PS-*b*-PEO to examine the morphology of the compatibilized blends. Taking into consideration the results obtained by DSC and DMA, only blends with 0.5 wt % HBC were studied. Images for blends without PS-*b*-PEO are reported in Figure 7. The uncompatibilized sPS-(DGEBA/MCDEA) blends show the typical characteristics of an immiscible blend. For 2.5 and 5 wt % sPS contents, the sPS phase dispersed in the epoxy matrix as spherical sPS spherulites with a size of 50–60 μm and distributed on the whole fractured surface can easily be observed [Figs. 7(a) and 7(b)]. As reported elsewhere,[18] these spherulites are formed by crystallization-induced phase separation of semicrystalline sPS (CIPS), grown from a homogeneous sPS-(DGEBA/MCDEA) reacting medium. Moreover, when observed in more detail [Figs. 7(c) and 7(d)], small sPS-rich particles with varying sizes of ~0.5–2 and ~0.5–4 μm for 2.5 and 5 wt % sPS, respectively, appear segregated from DGEBA/MCDEA matrix. These sPS-rich amorphous particles are probably the result of reaction-induced phase separation (RIPS). The interface between the sPS-rich particles and epoxy matrix is smooth and clear, suggesting a poor adhesion between the two phases, which is clearly shown in 3D AFM image in the Figure 7(e). The boundaries of the particles are well defined and separated from the matrix; furthermore, many spherical voids are observed in SEM images originated from the detachment of the sPS-rich particles during cryo-fracture process, indicating low interfacial adhesion.

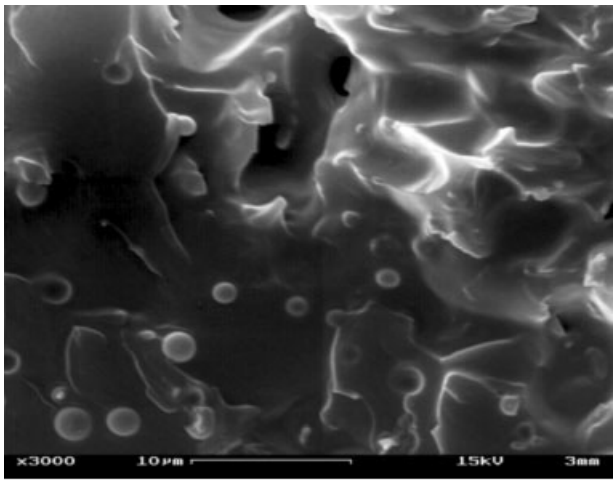

(a)

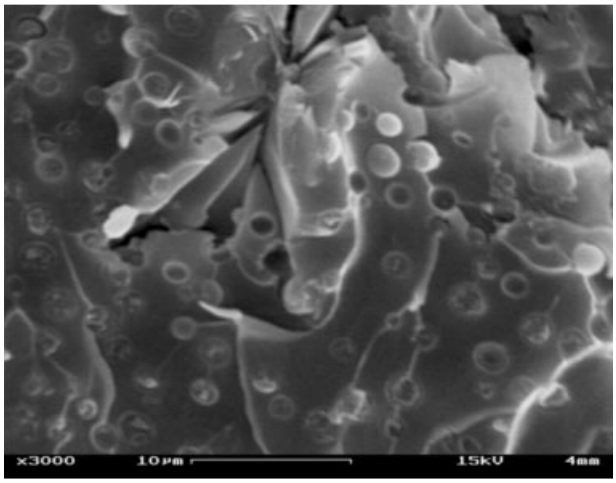

(b)

Figure 8 SEM micrographs of 5 wt % sPS-(DGEBA/MCDEA) cryo-fractured surface (a) without and (b) with 0.5 wt % of HBC.

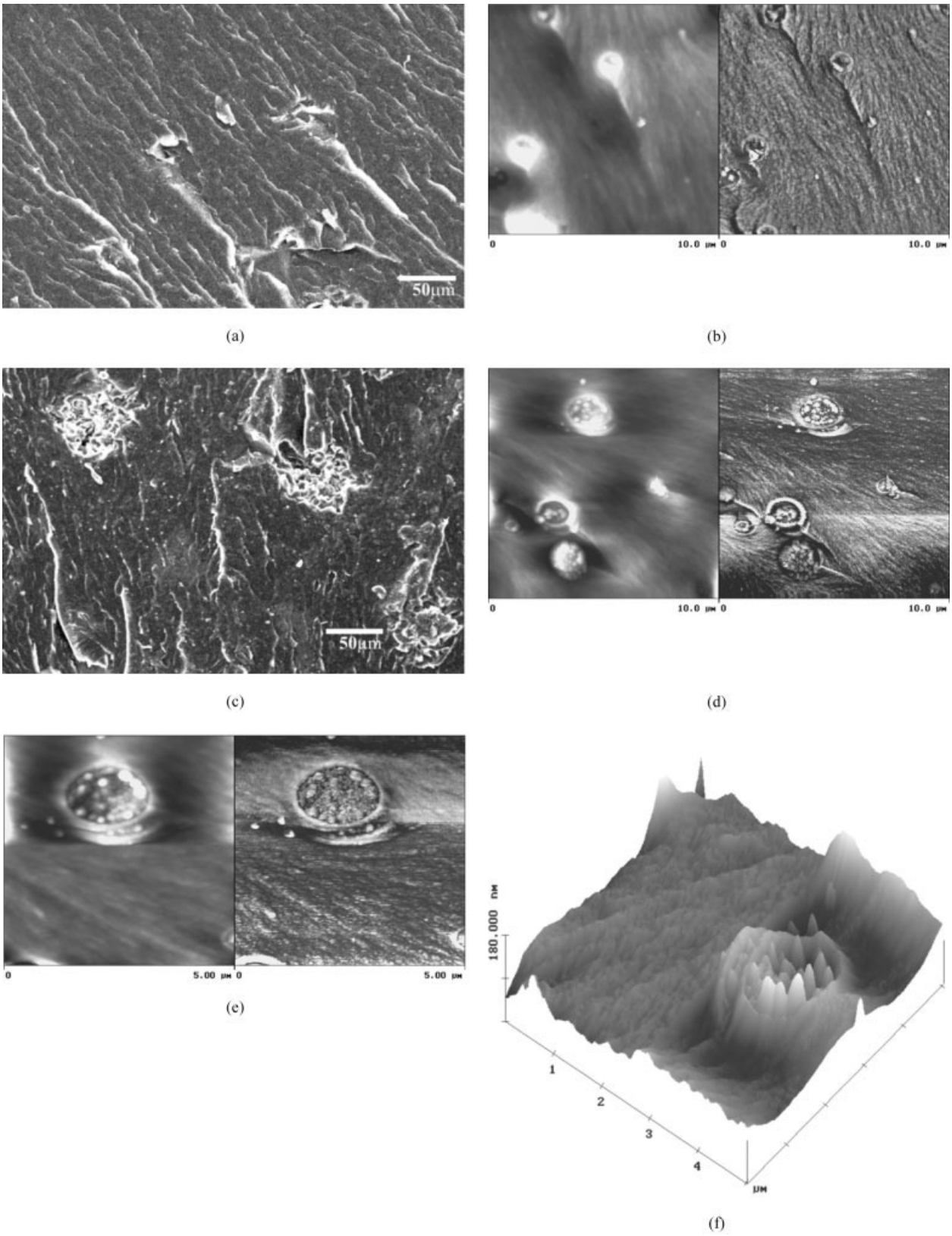

Figure 9 SEM and AFM micrographs of sPS-HBC-(DGEBA/MCDEA) cryo-fractured surface: (a) 2.5 wt % sPS 0.5 wt % HBC (×300), (b) 2.5 wt % sPS 0.5 wt % HBC (left/right: hight/phase AFM image), (c) 5 wt % sPS 0.5 wt % HBC (×300), (d) 5 wt % sPS 0.5 wt % HBC (left/right: hight/phase AFM image), (e) 5 wt % sPS 0.5 wt % HBC (left/right: hight/phase AFM image), (f) 5 wt % sPS 0.5 wt % HBC 3D AFM.

Those observations point out immiscibility, which is likely to stem the high interfacial tension occurring between components during network formation. In addition, uncompatibilized blends demonstrate a wide distribution in sPS-rich particles size, as shown in Figures 7(d) and 8(a). Blends containing 7.5 wt % sPS show typical cocontinuous morphology [Fig. 7(f)].

SEM and AFM micrographs carried on the cryofractured blends containing 2.5 and 5 wt % sPS and modified with 0.5 wt % PS-*b*-PEO are shown in Figures 8 and 9. The size of the dispersed spherical sPS spherulites does not change significantly in comparison with the systems without block copolymer. Nevertheless, it is worth to note that less spherulites of sPS appeared upon network formation [compare Figs. 7(a) and 7(b) with Figs. 9(a) and 9(c)]. As a consequence, the amount of amorphous sPS phase-separated from the epoxy matrix is higher than that for the blends without block copolymer, which can be clearly seen in Figures 8(a) and 8(b). Thus, for the compatibilized blends, the phase separation is induced by reaction instead of crystallization of sPS, as has been observed by dynamical–mechanical analysis and confirmed by hindrance of the crystallization of these blends expected by DSC. On the other hand, even if the average size is reduced insignificantly, the distribution of sPS-rich particle size becomes narrow showing also improvement of the dispersion of the separated phase (see Fig. 8), which is characteristic of compatibilization between immiscible polymer blends.[41,42] It is likely that during network formation, the presence of the PS-*b*-PEO lowers the interfacial tension between the components and improves the adhesion at the interface, as can be observed in 3D AFM image in Figure 9(f), especially it must be taken into account that the color height scale of AFM 3D image for this blend is more than ten times lower than that for blend without compatibilizer. During the network formation, compatibilizers reduce the surface tension, thus resulting in increasing the interfacial layer between sPS and epoxy phase and in a narrower distribution of the particles.

Both final morphologies of compatibilized blends and less tendency to crystallization for these blends, estimated by DSC, suggest that addition of adequate amount of diblock copolymer to the sPS-(DGEBA/MCDEA) blends can be effective in reducing the crystallization of sPS during network formation, thus RIPS becoming dominant.

CONCLUSIONS

sPS-(DGEBA/MCDEA) blends have been compatibilized by introduction of a small amount of PS-*b*-PEO diblock copolymers with different molecular weights.

On the basis of DMA and DSC results as well as SEM and AFM examinations, the introduction of 0.5 wt % HBC or LBC is beneficial for enhancing the compatibility between sPS and DGEBA/MCDEA phases in sPS-(DGEBA/MCDEA) blends containing 2.5 and 5 wt % sPS. Additionally, it was found that diblock copolymer with higher molecular weight of PS block (HBC) seems to be more effective compatibilizer than diblock copolymer with lower molecular weight of PS block (LBC). Taking into account that the ratio $M_{n,\mathrm{sPS}}/M_{n,\mathrm{PS}}$ is lower than one for HBC, while it is higher than one for LBC, the probability of compatibilization is also higher for HBC. Addition of 0.5 wt % HBC to sPS-(DGEBA/MCDEA) blends shifts the T_g of DGEBA/MCDEA phase to lower temperature, hinders the crystallization of sPS in blends, and generates morphologies with less spherulites of crystalline sPS phase and more particles of amorphous sPS. Addition of HBC decreases insignificantly the size of the sPS dispersed amorphous phase but also generates layers of HBC at the boundaries between components. Thus it is confirmed that in this case the compatibilizer works as surfactant and reduces the interfacial tension between sPS and DGEBA/MCDEA phases. Furthermore, the presence of HBC at the interface is confirmed by AFM microscopy. Addition of the compatibilizar to the sPS-(DGEBA/MCDEA) blend influences the final morphology of cured blend by changing in the prase separation mechanism, which occurs mostly by RIPS.

DMA analysis supports the lack of adhesion in the sPS-(DGEBA/MCDEA) systems and the compatibility effect in these systems with adequate amount of HBC or LBC added.

References

1. Po, R.; Cardi, N. Prog Polym Sci 1996, 21, 47.
2. Ishihara, N.; Seimiya, T.; Kuramoto, M.; Uoi, M. Macromolecules 1986, 19, 4264.
3. Candi, F. D.; Romano, G.; Russo, R.; Vittoria, V. Colloid Polym Sci 1990, 268, 720.
4. Cimmino, S.; Pace, E. D.; Martuscelli, E.; Silvestre, C. Polymer 1991, 32, 1080.
5. Cimmino, S.; Pace, E. D.; Martuscelli, E.; Silvestre, C. Polym Commun 1991, 32, 251.
6. Cimmino, S.; Pace, E. D.; Martuscelli, E.; Silvestre, C.; Rice, D. M.; Karasz, F. E. Polymer 1993, 34, 214.
7. Cimmino, S.; Pace, E. D.; Martuscelli, E.; Silvestre, C. Polymer 1993, 34, 2799.
8. Guerra, G.; Rosa, C. D.; Vitagliano, V. M.; Petraccone, V.; Corradini, P. Polym Commun 1991, 32, 30.
9. Hwang, S.-H.; Kim, Y.-S.; Cha, H.-C.; Jung, J.-C. Polymer 1999, 40, 5957.
10. Hwang, S.-H.; Kim, M.-J.; Jung, J.-C. Eur Polym J 2002, 38, 1881.
11. Bonnet, M.; Buhk, M.; Petermana, J. Polym Bull 1999, 42, 353.
12. Chiu, F.-Ch.; Peng, Ch.-G. Polymer 2002, 43, 4879.
13. Wang, Ch.; Chen, Ch. Ch.; Cheng, Y. W.; Liao, W. P.; Wang, M. L. Polymer 2002, 43, 5271.
14. Park, J.-Y.; Kwon, M. H.; Park, O. O. J Polym Sci Part B: Polym Phys 2000, 38, 3001.

15. Zafeiropoulos, N. E.; Schut, J.; Pohlers, A.; Stamm, M.; Gerard, J.-F. Macromol Symp 2003, 198, 345.
16. Schut, J.; Stamm, M.; Dumon, M.; Galy, J.; Gerard, J. F. Macromol Symp 2003, 202, 25.
17. Korenberg, C. F.; Kinloch, A. J.; Taylor, A. C.; Schut, J. J Mater Sci Lett 2003, 22, 507.
18. Tercjak, A.; Remiro, P. M.; Mondragon, I. Polym Eng Sci 2005, 45, 303.
19. Tercjak, A.; Serrano, E.; Remiro, P. M.; Mondragon, I. J Appl Polym Sci 2006, 100, 2348.
20. Noolandi, J.; Hong, K. M. Macromolecules 1984, 17, 153.
21. Choi, S. H.; Cho, I.; Kim, K. U. Polym J 1999, 31, 828.
22. Hong, B. K.; Jo, W. H. Polymer 2000, 41, 2069.
23. Chen, B.; Li, X.; Xu, S.; Tang, T.; Zhou, B.; Huang, B. Polymer 2002, 43, 953.
24. Abis, L.; Abbondanza, L.; Braglia, R.; Castellani, L.; Giannotta, G.; Po, R. Macromol Chem Phys 2000, 201, 1732.
25. Choi, W.-M.; Park, Ch.-I.; Park, O.; Lim, J.-G. J Appl Polym Sci 2002, 85, 2084.
26. Xu, S.; Chen, B.; Tang, T.; Huang, B. Polymer 1999, 40, 3399.
27. Jeon, H. K.; Feist, B. J.; Koh, S. B.; Chang, K.; Macosko, Ch. W.; Dion, R. P. Polymer 2004, 45, 197.
28. Girard-Reydet, E.; Sautereau, H.; Pascault, J. P. Polymer 1999, 40, 1677.
29. Girard-Reydet, E.; Sévignon, A.; Pascault, J. P.; Hoppe, C. E.; Galante, M. J., Oyanguren, P. A.; Williams, R. J. J Macromol Chem Phys 2002, 203, 947.
30. Leibler, L. Macromolecules 1982, 15, 1283.
31. Noolandi, J.; Hong, K. M. Macromolecules 1982, 15, 482.
32. Leibler, L. Makromol Chem Macromol Symp 1988, 16, 1.
33. Leibler, L. Physics A 1991, 172, 258.
34. Wenchun, H.; Koberstein, J. T.; Lingelser, J. P.; Gallot, Y. Macromolecules 1995, 28, 5209.
35. Paul, D. R.; Newman, S. Polymer Blends; Academic Press: New York, 1978.
36. Schut, J.; Stamm, M.; Dumon, M.; Gerard, J. F. Macromol Symp 2003, 198, 355.
37. Guo, Q.; Harrats, C.; Groeninckx, G.; Koch, M. H. J. Polymer 2001, 42, 4127.
38. Larrañaga, M.; Martin, M. D.; Gabilondo, N.; Kortaberria, G.; Corcuera, M. A.; Riccardi, C. C.; Mondragon, I. Polym Int 2004, 53, 1495.
39. De Candia, F.; Filho A. R.; Vittoria, V. Colloid Polym Sci 1991, 269, 650.
40. Ho, R. M.; Chang, Ch. Ch.; Chung, T. M.; Chiang, Y. W.; Wu, J. Y. Polymer 2003, 44, 1459.
41. George, S.; Neelakantan, N. R.; Varughese, K. T.; Thomas, S. J Polym Sci 1997, 35, 2309.
42. Willis, J. M.; Favis, B. D. Polym Eng Sci 1990, 30, 1073.